Zeitschrift: IABSE reports = Rapports AIPC = IVBH Berichte
Band: 37 (1982)

Artikel: Effect of root gap on the fatigue strength of welded joints
Autor: Sved, G. / Yeo, M.F. / Brooks, D.S.
DOI: https://doi.org/10.5169/seals-28906

Effect of Root Gap on the Fatigue Strength of Welded Joints

Effet du vide à la racine des joints soudés sur leur résistance à la fatigue

Einfluss des Zwischenraums an der Wurzel von Schweissverbindungen auf ihre Ermüdungsfestigkeit

G. SVED
The University of Adelaide
Adelaide, Australia

M.F. YEO
The University of Adelaide
Adelaide, Australia

D.S. BROOKS
The University of Adelaide
Adelaide, Australia

SUMMARY
The influence of root gaps on the static and fatigue strength of load bearing fillet welded members has been investigated using a finite element analysis, by strain gauging of large scale physical models, by testing of prototype models spark machined from solid plate, and by conducting static and low-cycle fatigue tests on real specimens. In the root gap range of 0 to 3 mm a defined reduction of fatigue strength with increasing gap was not revealed.

RESUME
L'influence du vide existant entre les pièces assemblées par cordon d'angle sur la résistance statique et à la fatigue d'éléments de construction soudés a été étudiée au moyen d'un calcul par éléments finis, au moyen de mesures de déformation par jauges d'extensométrie sur des modèles physiques à grande échelle, au moyen d'essais sur éprouvettes usinées tirées de la masse et érodées artificiellement, ainsi qu'au moyen d'essais statiques et de fatigue sous charge cyclique de pièces réelles. Pour des vides variant entre 0 et 3 mm, aucune réduction significative de la résistance à la fatigue n'a été constatée avec l'augmentation de l'écartement entre les pièces.

ZUSAMMENFASSUNG
Für geschweisste Kehlnahtverbindungen wurde der Einfluss des Spiels zwischen den Werkstücken auf die statische Festigkeit und den Ermüdungswiderstand untersucht. Dies erfolgte unter Anwendung eines Finite Element-Programmes sowie mit Hilfe von Deformationsmessungen an grossmassstäblichen Modellen und mit Versuchen an Prüflingen, die mittels Funkenerosion aus dem Grundmaterial hergestellt wurden. Zusätzlich erfolgten Versuche unter statischer und zyklischer Belastung an wirklichen Verbindungen. Für den Spielbereich von 0 bis 3 mm wurde keine bedeutende Abminderung der Ermüdungsfestigkeit mit zunehmendem Zwischenraum festgestellt.

INTRODUCTION

The cost of eliminating the gap in a weldment, as between the flange and the web of a built up I beam, can be very great. If - as our results so far indicate - a gap as big as one quarter of the nominal size of a fillet weld has no significant effect on the strength of the weldment, considerable savings can be effected in the preparation of welded joints.

In a previous study I.Tsuji and K. Ogawa (Ref.1) investigated "The effect of root gaps on the low cycle fatigue strength of cruciform welded joints". They investigated experimentally the effect of a gap varying from 0 to 3mm, and by finite elements found the stresses, using homogeneous material properties and a 1mm gap, with sloping end.

There are two effects that can alter considerably the results of a finite element analysis: the geometry of the weld, with the shape of the end of the root gap having a significant influence and metallurgical variations within the weld metal and in the heat affected zones.

To clarify the effect of these factors and of the assumption of plane stresses, it was decided to proceed with the investigation along five lines:

- Completing finite element calculations for differently shaped root gap ends and with due consideration to the variation of the mechanical properties in the weld metal and the heat affected zone.
- Manufacturing two models each 6 times full scale, machined from 10mm steel plate, one with 1mm and one with 11mm root gap. These models were strain gauged and tested statically. The results of these tests will be reported separately.
- Constructing prototype size models, with slots machined by spark erosion from solid plate, to allow geometrical effects to be investigated separately from any interfering metallurgical effects.
- Carrying out low cycle fatigue tests on conventional welded specimens.
- Cutting specimens of varying thickness (4,8,16,32,64mm) from adjoining parts of a long cruciform section weldment and fatigue testing these specimens with forces proportional to their thickness.

Visual inspection indicated that the shape of the end of the root gap was curved in some cases, straight in others. The curved end could be convex or concave, while the straight end could include an angle that varied through 90^{o}, i.e. between 45^{o} either side of the load axis.

The variation of the mechanical properties was investigated by taking hardness traverses across the weldments; these indicated the hardness varied by as much as 50 per cent within the area where yielding was expected.

The specimens used - calculation of stresses

The basic specimen used is shown in Figure 1. Each of the welded specimens was sliced from a 1 metre long weldment that had a tapered gap. A semi automatic gas shielded (CO_2) process was used - typically for an 8mm weld the weld parameters were 325A, 28V, with a welding speed of 255mm/min for zero gap. One leg length was kept constant, equal to the nominal size of the weld (6 or 8mm); the length of the other gap was increased to compensate for the gap.(See Figure 2). The welding speed was decreased with increasing gap - in a typical case the average speed was 225mm/min for a 1 metre long weldment.

The variable weld geometry had some effect on the calculated stresses.

Resolving the force acting on one weld ($P/_2$) into components normal and parallel to the minimum throat (for notation, refer to Figure 2) gives

$$\sigma_n = \frac{F_n}{\ell t} = \frac{P}{2} \cdot \frac{b}{d} \cdot \frac{1}{\ell t} \quad ; \quad \tau = \frac{F_t}{\ell t} = \frac{P}{2} \cdot \frac{t}{d} \cdot \frac{1}{\ell t} = \frac{P}{2d\ell}$$

The von Mises yield criterion is

$$\sigma_{eff} = (\sigma_n^2 + 3\tau^2)^{\frac{1}{2}} = \frac{P}{2d\ell}\left[\left(\frac{b}{\ell}\right)^2 + 3\right]^{\frac{1}{2}}$$

which reduces to

$$\sigma_{eff} = \frac{P}{2d\ell}\left[\left(\frac{d+\ell}{d}\right)^2+3\right]^{\frac{1}{2}} = \frac{P}{d\ell}\left[1 + \frac{\ell}{2d} + \left(\frac{\ell}{2d}\right)^2\right]^{\frac{1}{2}} \simeq \frac{P}{d\ell}\left(1 + \frac{\ell}{4d}\right) \ldots . \quad (1)$$

The last approximation introduces an error of less than 7% even for $\ell/d = \frac{1}{4}$ -an error which is small compared with all other approximations involved. In addition, an error on the safe side is caused by the throat thickness being considerably larger than the nominal one in most cases due to the weld penetration into the gap.

The stresses quoted in this report are generally the nominal stresses, calculated from equation (1) setting ℓ=o. However, equation (1) can be used to explain partially the relatively small effect of a root gap - the other explanation being the improved stress-flow (reduced stress concentration factor) associated with the smaller re-entrant angle at the toe of the weld.

Finite element analysis

Only the part shaded in Figure 1 was modelled by finite elements. A typical mesh layout is shown in Figure 3. The boundary conditions assumed were roller supports at nodes along edges AJ and JHGF, to account for symmetry, free nodes along BA and uniform axial displacement due to axial loading for all nodes along edge FE.

A strain hardening material was assumed; the stress-strain curve was approximated by four straight lines (Figure 4). The first, passing through the origin and terminating at a point M, had a slope of E=200 000 MPa; M corresponded to the initial yield point. The yield stress, σ_y, had five different values (σ_y = 250,270,310,350,390 MPa),to be used in different zones, established by the previously mentioned hardness traverse of the weld and of the heat affected zone. The second straight line, MN, terminated at a stress of (σ_y+ 5) MPa and a strain of 1.5%: the third straight line, NP, had a slope of 5000 MPa and terminated at a stress of $2\sigma_y$, while the last part, PR, terminated at a stress of σult = ($2\sigma_y$ + 5) MPa and a strain of 15%. At points where the stresses were multiaxial, the same relationships were assumed to hold between "effective stress" and "effective strain" increments; these were defined as the octahedral shearing stress and the octahedral shearing strain respectively.

The elastic-plastic analysis followed the "initial stress" approach.(Ref.2). Conventional shape functions were used for the 8 noded curved quadrilateral isoparametric elements employed; the material property matrix corresponded to the current value of effective strain. All integrals were evaluated by 3 x 3 Gaussian quadrature.

As a first step, the elastic stiffnesses were used to evaluate the elastic stress distribution corresponding to an arbitrary value of the (equal) displacement of the nodes along FE. These displacements and the corresponding strains and stresses were scaled to cause yield at the relatively highest stressed point taking into account different zones had different yield strengths. The analysis

was continued by applying equal increments of displacements in steps of 0.01mm to all nodes along FE. Using the previously established stiffness matrix, an extrapolated set of values was calculated for all increments in nodal displacements, nodal forces, stresses and strains. For all elements, for which the effective stress value exceeded the yield strength, an updated stiffness matrix was calculated, using the current material property matrix to conform with the stress-strain incremental values. The problem was re-solved, using the updated stiffness matrix; if the differences between the extrapolated and the re-calculated values exceeded a pre-selected convergence criterion, the process was repeated iteratively until the "residual nodal forces" fell below a convergence value. Usually five iterations were sufficient to allow applying the next increment.

Geometrical non-linearities caused by the relatively large displacements can be allowed for by adding the displacements to the nodal coordinates and re-calculating the element characteristics for the altered geometry.

The calculations were terminated when the effective strain reached the "failure" value of 15% at any one point.

Extensive use was made of graphical output facilities to avoid the collection of excessive amount of data that would be hard to scan and to interpret. In the elastic range the principal stresses were plotted by the computer at the central Gauss point of every element. In the elastic-plastic range an x was printed at every Gauss point that reached the plastic range (point M on the stress-strain curve); This was changed to a + when the effective strain reached 1.5% (point N) and to a <> when the effective stress reached $2\sigma_y$(point P). A typical output is shown in Figure 3.

Five different profiles were analysed with a 3mm gap, using slopes for the end of the gap that varied from approximately 30^0 to 55^0 with the load axis, both in the"positive" and "negative" directions. In addition square gap ends with 3,2, 1 and 0mm opening were analysed. For the zero gap nodes on the two sides of the gap (initially coincident) were allowed to move independently.

Typical calculated load-extension graphs are shown in Figure 5; the letters M, N,P, and R correspond to the previously described points on the stress-strain graph.

Conclusions from the finite element analysis

- First yielding, which was reached at approximately the same load for all gap and configuration, was always at the root of the gap (point A on Figure 3),but it was followed very closely by yielding at the toe (point B) and after a few increments of elongation at points C and D.
- After approximately 10 increments there was a continuous yielded zone between points A and B; this zone was quite extensive by the 17th step.
- The maximum load reached was 49kN±6kN, except for the square end 3mm gap (37.7kN).
- Six calculations reached "failure" after 45±7 elongation increments; exceptions were two square ended gaps (for 3mm 30 steps, for 1mm 32 steps) and one with end sloping at 30^0 (87 steps).

Fatigue tests on spark eroded specimens

Seven fatigue specimens, machined from 6mm plate to the outline shown in Figure 1, had spark eroded slots to investigate geometrical effects, free from metallurgical changes introduced by the welding process. The "weld profiles"

corresponded to a 6mm fillet weld. The fatigue tests were carried out in an Instron servo-controlled machine, under load control, at a rate of 2-3Hz. The results are summarized in Table 1.

TABLE 1.

Fatigue tests on spark eroded specimens-6mm plate, 6mm weld profile			
Specimen	Load range(kN)	Cycles to failure	Shape of end of gap
1	0.8 - 10	42720	Semi-circular
2	0.8 - 10	45110	Semi-circular
3	0.8 - 10	53290	Quarter circle
4	0.8 - 10	60580	45° slope
5	0.8 - 12	15600	Square-0.5mm gap
6	0.8 - 12	15170	Square-0.75mm gap
7	0.8 - 12	11160	Square-1.25mm gap

Specimens 1-4 had extensometers fitted across the gap. For the first two no increase in the extensometer readings were noted in the first 20 000 cycles; for specimens 3 and 4 the readings were constant until 30 000 cycles were applied.

In the second series square ended slots were spark eroded in blanks machined from 8mm plate. Results are shown in Table 2.

TABLE 2.

Fatigue cracks in specimens with rectangular spark eroded slots;8mm plate, 6mm weld profile. Load range 0.8-12kN, except for specimen No.8			
Specimen	Gap (mm)	Cycles to failure	Remarks
8	2.15	256 000 29 400	0.8 - 10kN 0.8 - 12kN 3 cracks
9	2.15	36 200	3 cracks
10	2.15	35 160	4 cracks
11	1.5	22 200	
12	1.35	22 400	
13	1.3	13 520	1 crack

Tests on large scale models

Two large scale models (6 times full size) were machined from 10mm mild steel plate. One model had a 1mm wide gap, the other a 11mm gap, both with square ends. These models were tested statically, after extensive strain gauging. Results will be reported elsewhere.

Fatigue tests on welded specimens

Test specimens were cut from 1 metre long weldments to avoid end effects. These were made with tapering gaps; the actual gap in any one specimen was measured with feeler gauges.

The first weldment had a significant gap on one side of the cross bar only; all specimens failed at the gap. The results are shown in Table 3.

TABLE 3.

Fatigue life of welded specimens-8mm thick - 8mm nominal weld. Load range 0.8kN - 28kN.			
Specimen	Gap(mm)	Cycles to failure	Fatigue cracks
14	0.45	44 300	2 at end of gap, 1 at toe
15	0.5	84 740	2 at end of gap, 1 at toe
16	0.6	43 210	2 at end of gap
17	0.7	25 900	2 at end of gap
18	0.85	65 620	2 at end of gap, 1 at toe
19	0.9	59 880	2 at end of gap, 1 at toe

The results for the specimens cut from the second weldment are shown in Table 4. In this case there were significant (although different) gaps on the two sides of the cross bar. The gap that failed is indicated by underscoring.

TABLE 4.

Fatigue life of welded specimens - 8mm thick - 8mm nominal weld Load range 0.8kN - 28kN.			
Specimen	Gap(mm)	Cycles to failure	Fatigue cracks
20	.02/.6	29 300	1 at end of gap
21	.05/1.5	33 420	Fracture across throat
22	.5/2.15	72 080	2 at end of gap, 1 at toe
23	.7/1.15	57 520	2 at end of gap, 1 at toe
24	1.0/1.3	78 810	2 at end of gap
25	1.2/2.4	73 550	2 at end of gap

In the third series a weldment with tapering gaps was sliced into 20 test pieces. These formed 4 series, each comprising 5 specimens, cut from adjoining parts of the weldment, with thicknesses of 4,8,16,32 and 64mm, to investigate the effect of triaxiality in long welds. The results of these tests are shown in Table 5.

TABLE 5. TEST RESULTS

Size Load(kN)	4mm 10.5	8mm 21	16mm 42	32mm 84	64mm 168	Average
Series A	1.1 1.8 2R 296050	1.2 1.9 2R 293600	1.2 2R 2.1 R 267750	1.1 2R 2.0 262280	1.3 2.3 2R 292423	282420 ±14360
B	0.9 2R T 1.35 171480	0.8 1.4 R 201580	0.8 1.5 2R 175500	0.7 2R 1.5 230725	0.9 R 1.6 227300	201315 ±24890
C	-	0.2 2R 1.1 122850	0.4 2R 1.0 T 129760	0 2R 0.95 187130	0.6 R 1.25 184260	156000 ±29810
D	0 0.2 2R 152050	0 0.15 2R 138930	0 0.15 2R 208625	0 0.1 2R 145270	0.1 2R 0.8 144010	157780 ±25765
Average	206000 ±63800	189240 ±67050	195400 ±50280	206350 ±44220	212000 ±55000	

{see over}

In Table 5, the entries show the following information:
(1) Size of gaps on test piece
(2) Gap size on the side at which failure occurred is indicated by underlining
(3) Mode of failure: R - root failure; 2R - root failure at both ends of the gap; T - toe failure
(4) Cycles to failure
(5) Averages and standard deviations, for both specimen sizes and for series.

CONCLUSIONS

- Results so far are restricted to relatively high stress, low fatigue life conditions.
- Neither the finite element calculations, nor the low cycle fatigue tests showed a significant reduction of strength with increasing gap size in the range investigated.
- The finite element calculations indicated that the stress levels at the toe of the weld were slightly lower than the stresses at the end of the root gap.
- The fatigue tests indicated that in many cases cracks could be seen to propogate from the end of the gap and from the toe of the weld before the specimen fractured.
- The tests on the specimens spark-eroded from the solid showed that the geometry of the gap-end had a considerable effect on the fatigue life of the specimen.
- The length of the weld (the thickness of the specimen) had no significant effect on the fatigue strength of the weld.

ACKNOWLEDGEMENTS

The research was supported by a grant from the Australian Welding Research Association; the welded specimens were provided by Johns Perry - Perry Engineering Division, Adelaide, South Australia.

REFERENCES

- I. TSUJI and K. OGAWA, "The Effect of Root Gaps on Low Cycle Fatigue Strength of Cruciform Welded Joints", Trans. of the Japan Welding Soc., vol. 7, April 1976.
- O.C.ZIENKIEWICZ,"The Finite Element Method" McGraw Hill 1977.

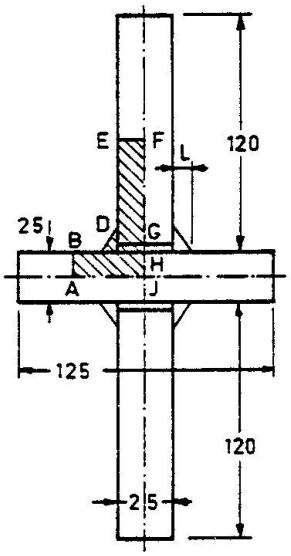

FIGURE 1. TEST SPECIMEN

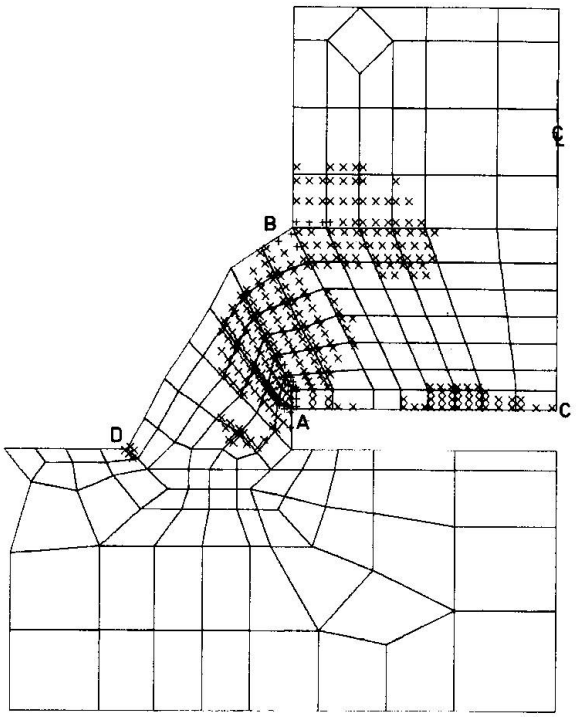

FIGURE 3. MESH ARRANGEMENT AND YIELD PATTERN

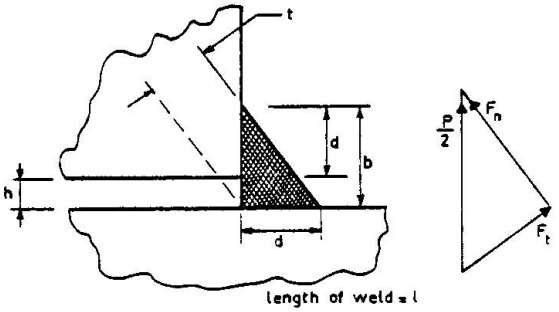

FIGURE 2. WELD GEOMETRY

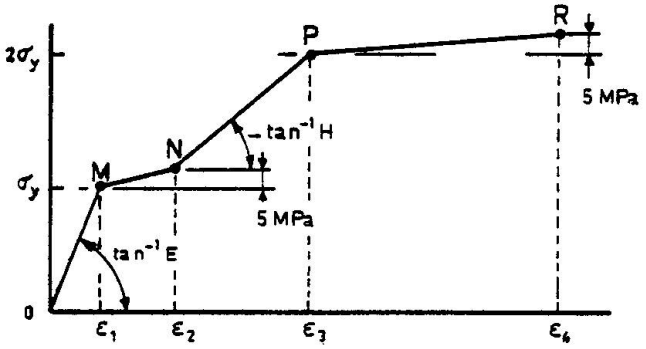

FIGURE 4. IDEALIZED STRESS_STRAIN RELATIONSHIP

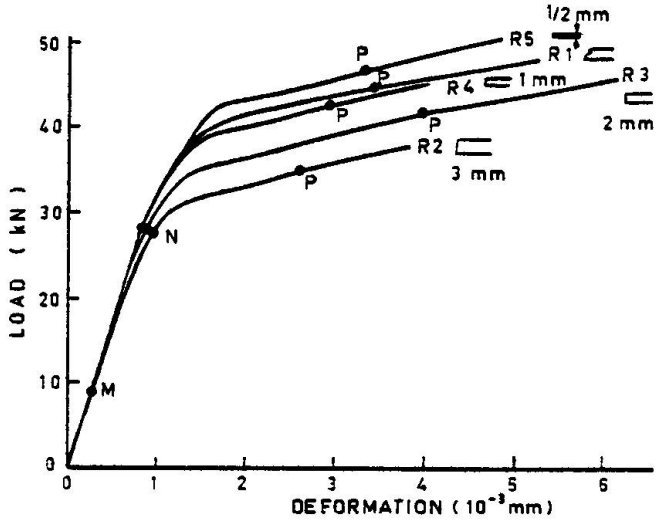

FIGURE 5. LOAD_ELONGATION CURVES OBTAINED FROM COMPUTED RESULTS